

ANALYTICAL MODEL FOR CFRP SHEETS BONDED TO CONCRETE

Brian Miller and Dr. Antonio Nanni
University of Missouri – Rolla
Department of Civil Engineering
225 ERL 1870 Miner Circle
Rolla, MO 65401, USA

Dr. Charles E. Bakis
Pennsylvania State University
Dept. of Engr. Science & Mechanics
227 Hammond Building
University Park, PA 16802, USA

KEYWORDS: bond, CFRP, composites, concrete, externally bonded reinforcement, laminate, peeling, repair

ABSTRACT

Carbon Fiber Reinforced Polymer (CFRP) sheets are used as externally bonded reinforcement for concrete structures to improve flexural and shear strength and confinement of concrete. The bond between CFRP sheets and concrete is important. It is the means for the transfer of stress between the concrete and CFRP in order to develop composite action. An experimental investigation was conducted in order to determine the effect of bonded length, concrete strength, and number of plies (stiffness) of CFRP sheets on bond. An analytical model was developed using this experimental data. The model is briefly discussed in terms of its application to design.

INTRODUCTION

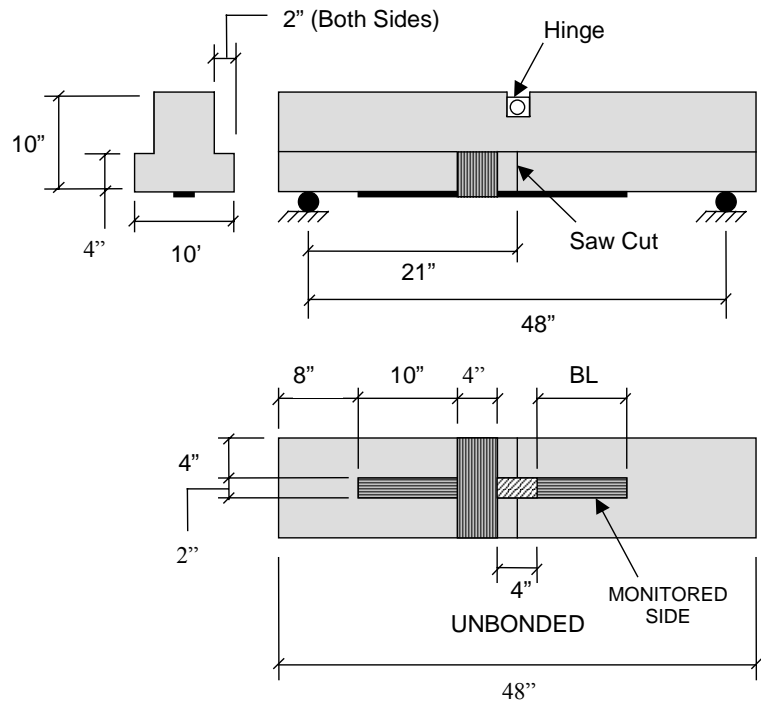
The use of FRP for reinforcement for concrete structures has emerged as an exciting and promising technology in materials and structural engineering. In particular, the use of CFRP sheets as externally bonded reinforcement has potential in the area of repair/rehabilitation of concrete structures (Nanni, 1997).

The bond between CFRP sheets and concrete is an issue that must be addressed in order to achieve safe and properly designed structures. The importance of bond is that it is the means for the transfer of stress between the concrete and CFRP in order to develop composite action. The bond must be characterized by determining the shape of the strain distribution in the CFRP sheet and the factors that affect the strain distribution.

It is known that when using externally bonded CFRP sheets, premature failure known as peeling can occur at levels of stress much lower than the ultimate strength of the CFRP. Equations are needed to address this type of failure in design.

OUTLINE OF EXPERIMENT

Test specimens were prepared to address the factors that were expected to affect the bond. In this project, bonded length, concrete strength, and number of plies (stiffness) of CFRP were addressed. The testing in this project was performed on the specimen shown in Figure 1. The specimen is a plain concrete beam with inverted T-shape. It had a simply supported span of 42 in (1067 mm) and a total length of 48 in (1219 mm). A CFRP strip was bonded to the tension face of the beam. The sheet was 2 in (51 mm) wide and had a fiber thickness of 0.0065 in (0.165 mm). The modulus of elasticity of the fiber is 33000 ksi (228 GPa) and the tensile strength is 550 ksi (3.8 GPa). Table 1 shows the specimens that were tested. For a more detailed description of the experimental program, refer to (Miller, 1999).



Note: 1 in = 25.4 mm

Figure 1: Test Specimen

Table 1: Description of Specimens

Series Number	Specimen Code	Concrete Class [f'_c] (psi)*	Number of Plies	Bonded Length (in)
I	6-1-4-1	6000 [6860]	1	4
	6-1-4-2			8
	6-1-8-1			12
	6-1-8-2			12
II	6-2-4-1	6000 [5900]	2	4
	6-2-4-2			8
	6-2-8-1			12
	6-2-8-2			12
III	3-1-4-1	3000 [3550]	1	4
	3-1-4-2			8
	3-1-8-1			12
	3-1-8-2			12
	3-1-12-1			12
	3-1-12-2			12

*Top number is class of concrete while 28-day strength is shown in brackets

Note: 1 in = 25.4 mm; 1 psi = 6.89 kPa

EXPERIMENTAL RESULTS

Table 2 shows a sample of the test results. It was found that the ultimate load of the specimens was the same for all of the bonded lengths. The reason the bonded length did not affect the ultimate load is the existence of an *effective bond length*. The length of sheet from the point of maximum stress to the point where the stress decreases to zero is known as the effective bond length. If the bonded length is greater than the effective bond length, the bonded length will have no effect on the ultimate load if the failure mode of the specimens is by peeling of the CFRP sheet.

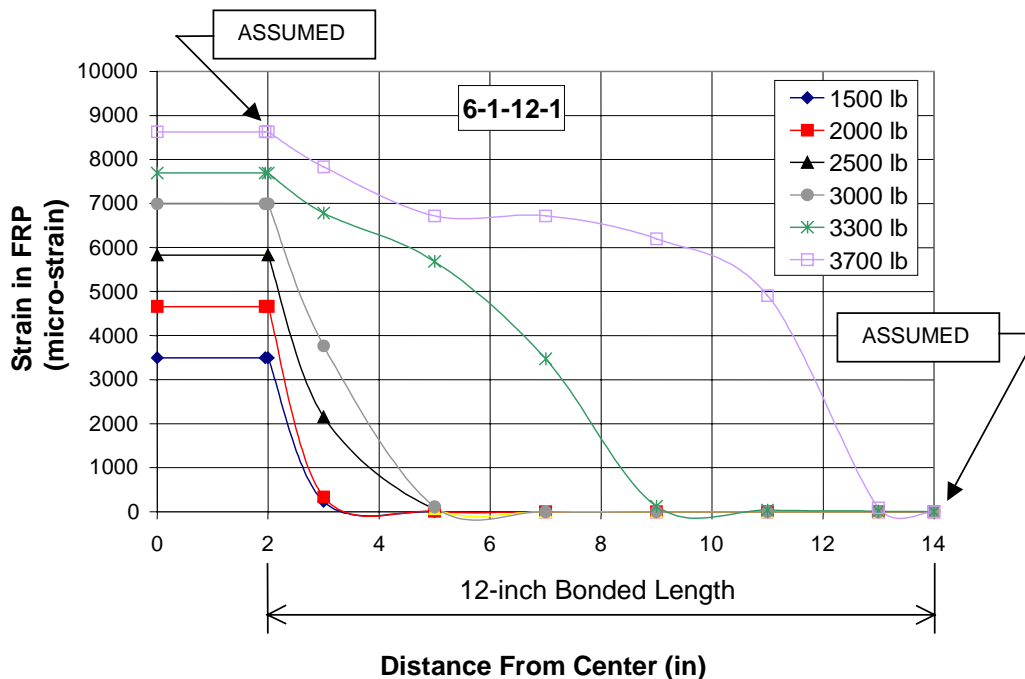
In this project, the peeling begins at midspan of the specimen and is shown in

Figure 2. Miller (1999) describes the mechanism of the peeling failure mode in detail.

Table 2: Experimental Results

Series I Specimens	Ultimate Load (lb)	Series II Specimens	Ultimate Load (lb)	Series III Specimens	Ultimate Load (lb)
6-1-4-1	3720	6-2-4-1	5930	3-1-4-1	3300
6-1-4-2	3990	6-2-4-2	5140	3-1-4-2	3120
6-1-8-1	3560	6-2-8-1	4630	3-1-8-1	4450
6-1-8-2	3190	6-2-8-2	6260	3-1-8-2	2920
6-1-12-1	3830	6-2-12-1	5590	3-1-12-1	4770
6-1-12-2	3390	6-2-12-2	5080	3-1-12-2	3450
Average	3613	Average	5438	Average	3668
Standard Deviation	294	Standard Deviation	602	Standard Deviation	757
Coefficient of Variation	8.14%	Coefficient of Variation	11.07%	Coefficient of Variation	20.65%

Note: 1 lb = 4.45 N



Note: 1 in = 25.4 mm; 1 lb = 4.45 N

Figure 2: Strain Distribution

The concrete strength also did not affect the ultimate load of the specimens. The reason the concrete strength had no effect was because the peeling failure occurred in the concrete-epoxy interface.

The number of plies of CFRP sheet did affect the ultimate load. It was found that the ultimate load increased when the number of plies was increased. Based on the change of the number of plies (stiffness), a model was developed to predict the ultimate load of the specimen.

ANALYTICAL MODEL

The first step in developing the model was to quantify the effective bond length of the sheet. This was accomplished by utilizing the linear shape of the strain distribution at the ultimate stage. Maeda et al. (1997) and Brosens and Van Gemert (1997) also noted the linear shape of the strain distribution at the ultimate stage. Experimentally, for each specimen a value of the slope ($d\varepsilon/dx$) of the linear portion of the strain location curve was found. The curves used to calculate the slopes are shown in

Figure 3 and Figure 4 for Series I and II respectively. The curves chosen were the strain distributions just before peeling occurred. It should be noted that the value of zero on the x-axis corresponds to the start of the bonded region. The values of $d\varepsilon/dx$ are shown in Table 3. As can be seen, the value for $d\varepsilon/dx$ is larger for Series I than Series II. Also shown in these two tables is the load that corresponds to the curve from which $d\varepsilon/dx$ was obtained. The strain was then calculated from the load using equation (1), and the effective bond length, L_e , was then calculated by equation (2). The values for 6-1-4-2 were not used in the calculation for the average, standard deviation, and coefficient of variation for Series I. Likewise, 6-2-4-1 and 6-2-4-2 were not used in the calculations for Series II. The reason for this was because the value of $d\varepsilon/dx$ for these specimens was considerably different as compared to the other specimens of the series. The values of the coefficient of variation based on the remaining specimens show that the results are consistent. It was found that the effective bond length for Series I and II are close to the same.

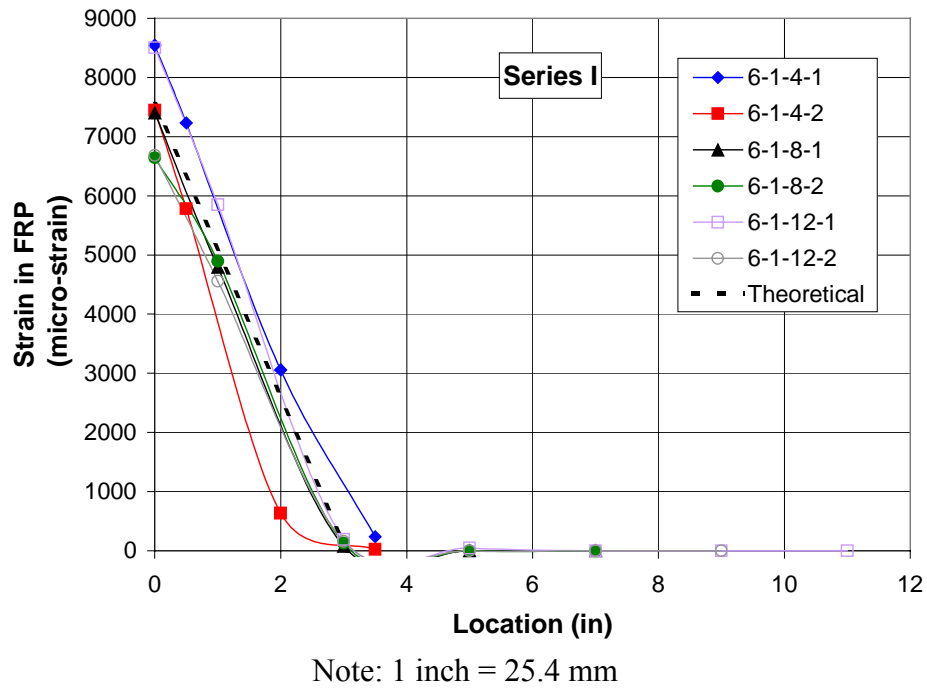


Figure 3: Curves Used to Calculate $d\epsilon/dx$ for Series I

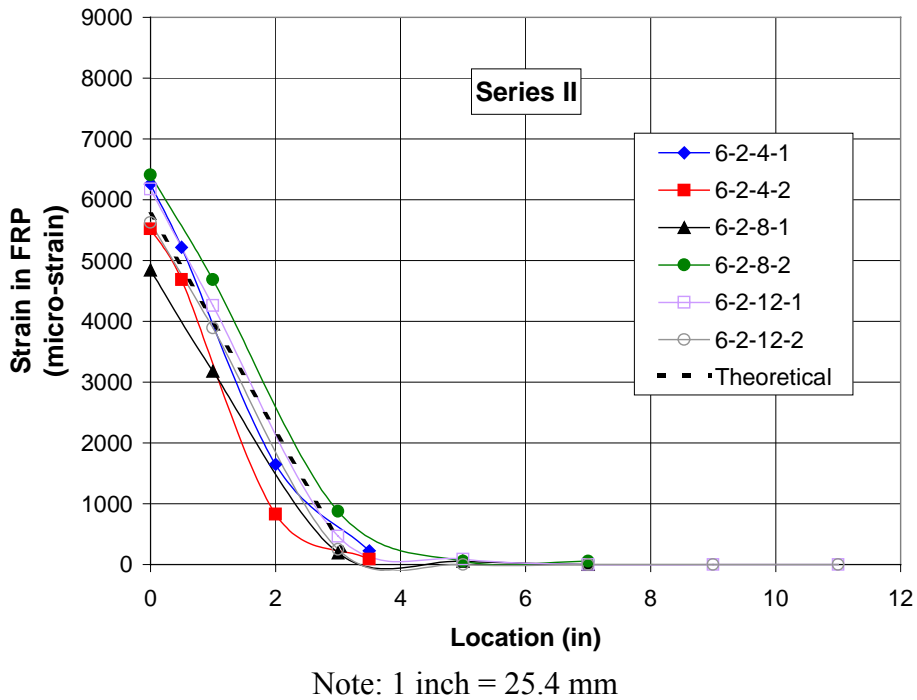


Figure 4: Curves Used to Calculate $d\epsilon/dx$ for Series II

Table 3: Values Used to Find L_e

Specimen	Load	$d\epsilon/dx$	ϵ_{max}	L_e	Specimen	Load	$d\epsilon/dx$	ϵ_{max}	L_e
----------	------	----------------	------------------	-------	----------	------	----------------	------------------	-------

	(lb)	(μ/in)	(με)	(in)		(lb)	(μ/in)	(με)	(in)
6-1-4-1	3666	2753	8545	3.10	6-2-4-1	5372	2323	6261	2.70
6-1-4-2	3190	3410	7436	2.18	6-2-4-2	4736	2397	5520	2.30
6-1-8-1	3176	2429	7403	3.05	6-2-8-1	4156	1542	4844	3.14
6-1-8-2	2850	2207	6643	3.01	6-2-8-2	5499	1853	6409	3.46
6-1-12-1	3650	2280	8508	3.06	6-2-12-1	5300	1903	6177	3.25
6-1-12-2	2867	2179	6683	3.07	6-2-12-2	4830	1796	5629	3.13
Average	3242	2470	7557	3.06	Average	4946	1774	5765	3.25
Standard Deviation	402	275	936	0.034	Standard Deviation	597	160	696	0.15
Coefficient of Variation	12.4%	11.1%	12.4%	1.1%	Coefficient of Variation	12.1%	9.0%	12.1%	4.7%

Note: 1 lb = 4.45 N; 1 in = 25.4 mm Not Considered

$$\varepsilon_{\max} = \frac{P_{\max}}{nt_f w_f E_f} \times 10^6 \quad (1)$$

$$L_{e-\text{exp}} = \frac{\varepsilon_{\max}}{\left(\frac{d\varepsilon}{dx}\right)} \quad (2)$$

ε_{\max} = Strain corresponding to ultimate load (με)

P_{\max} = Ultimate load (kips or kN)

n = Number of plies

t_f = thickness of CFRP sheet (in or mm)

E_f = Modulus of Elasticity (ksi or GPa)

w_f = width of CFRP sheet (in or mm)

$L_{e-\text{exp}}$ = Effective bond length found experimentally (in or mm)

$(d\varepsilon/dx)$ = Slope of the strain distribution curve (μ/in or μ/mm)

The values for L_e shown in Table 3 were plotted versus the stiffness of the CFRP sheet and can be seen in Figure 5. The axial stiffness of a material is defined as the cross-sectional area multiplied by the tensile modulus of the sheet. However, for FRP sheets a unit width is often considered and the stiffness is considered the thickness multiplied by the tensile modulus. An analytical model developed by Maeda et al. (1997) is shown in equation (3). It was found that the results from Maeda et al. (1997) does not agree with the results presented by the current project. The reason for this is that Maeda et al. (1997) considered an average value for $d\varepsilon/dx$ for all stiffnesses. From this they calculated the effective bond length from equation (2). The problem with this approach is that since the maximum strain will decrease as the stiffness increases, the effective bond length also decreases. However, the data from this project seems to indicate that $d\varepsilon/dx$ decreases as the stiffness increases. Since the strain decreases also, the effective bond length stays constant. Therefore, it seems to be more appropriate to set the effective bond length to a constant and develop an equation for $d\varepsilon/dx$. Until more testing can be conducted, the

conservative value of L_e may be assumed to be 3 in (76 mm). The values of $d\varepsilon/dx$ are plotted in Figure 6. A linear approximation is also plotted. Equation (4) is the equation for this line.

$$L_{e-M} = \frac{\exp\left[6.134 - 0.58 \ln\left(\frac{nt_f \times E_f}{5.71}\right)\right]}{25.4} \quad (3)$$

$$L_{e-M} = \exp[6.134 - 0.58 \ln(nt_f E_f)] \quad (3M)$$

L_{e-M} = Effective bond length calculated by Maeda et al. (1997) (in or mm)

$$\frac{d\varepsilon}{dx} = -2.915(nt_f E_f) + 3024 \quad (4)$$

$$\frac{d\varepsilon}{dx} = -0.654(nt_f E_f) + 119.06 \quad (4M)$$

Note for equations (3) and (4), the units for t_f is in. and E_f is ksi. In equation (3M) and (4M), the units for t_f is mm and E_f is GPa.

If the bond stress, τ , is taken as the average bond stress over the effective bonded length, the force P can be expressed by equation (5). Also, equation (5) can be rewritten in terms of stress as shown by equation (6).

$$P_{\max} = \tau \times L_e \times w_f \quad (5)$$

$$f_{fp} = \frac{\tau L_e}{nt_f} \quad (6)$$

f_{fp} = peeling stress of the FRP (ksi or GPa)

The shear stress, τ , can be found by equilibrium of forces from

Figure 7 as shown in equation (7).

$$P_1 - P_2 = \tau w_f dx \quad (7)$$

The force P can be expressed in terms of strain as in equation (8). Equation (8) can be substituted into equation (7) and noting that E_f , t_f , and w_f are constant gives equation (9).

$$P = nt_f w_f \varepsilon_f E_f \quad (8)$$

$$(\varepsilon_1 - \varepsilon_2) E_f nt_f w_f = \tau w_f dx \quad (9)$$

$(\varepsilon_1 - \varepsilon_2)$ can be expressed as shown in equation (10). Substituting (10) into (9) and solving for τ gives equation (11).

$$(\varepsilon_1 - \varepsilon_2) = \Delta\varepsilon = d\varepsilon \tag{10}$$

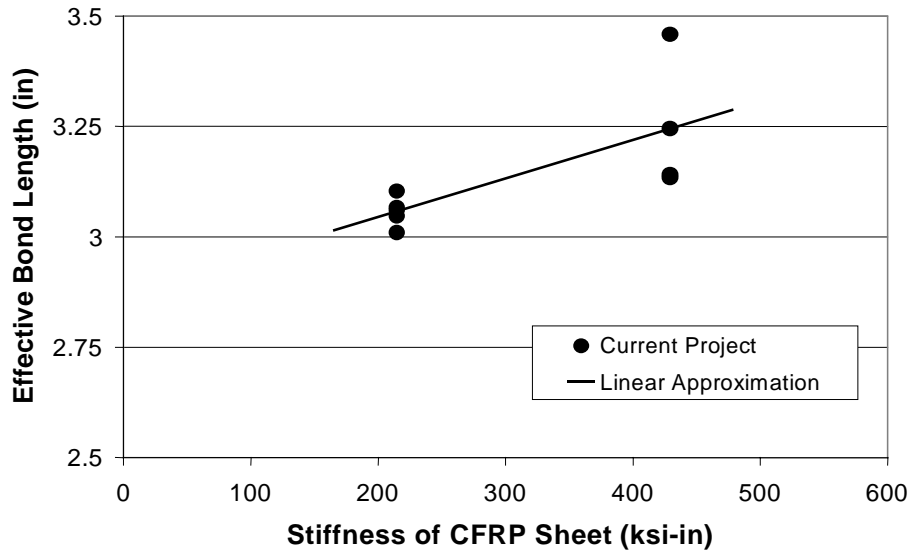
$$\tau = nt_f E_f \left(\frac{d\varepsilon}{dx} \right) \times 10^{-6} \tag{11}$$

τ = Average bond stress (ksi or GPa)

Substituting equation (4) into equation (11) gives equation (12). Note that for equation (12) t_f has units of in and E_f has units of ksi, and for (12M) t_f has units of mm and E_f has units of GPa.

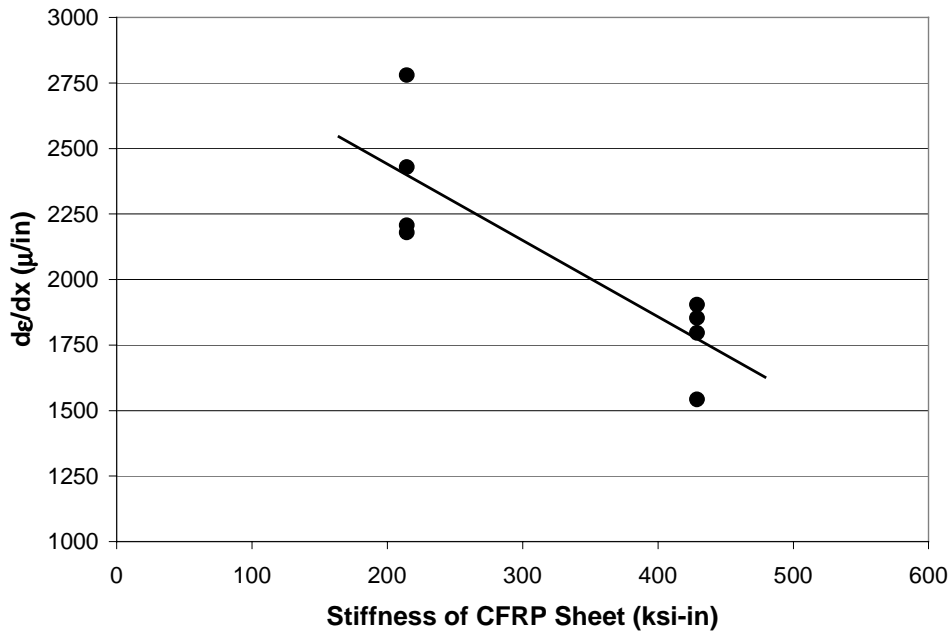
$$\tau = [-2.915(nt_f E_f)^2 + 3024(nt_f E_f)] \times 10^{-6} \tag{12}$$

$$\tau = [-0.654(nt_f E_f)^2 + 119.06(nt_f E_f)] \times 10^{-6} \tag{12M}$$



Note: 1 inch = 25.4 mm; 1ksi-in = 5.71 GPa-mm

Figure 5: Effective Bond Length vs. Stiffness



Note: 1 inch = 25.4 mm; 1ksi-in = 5.71 GPa-mm

Figure 6: $d\epsilon/dx$ vs. Stiffness

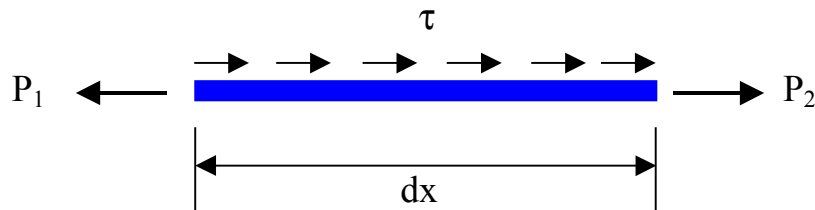


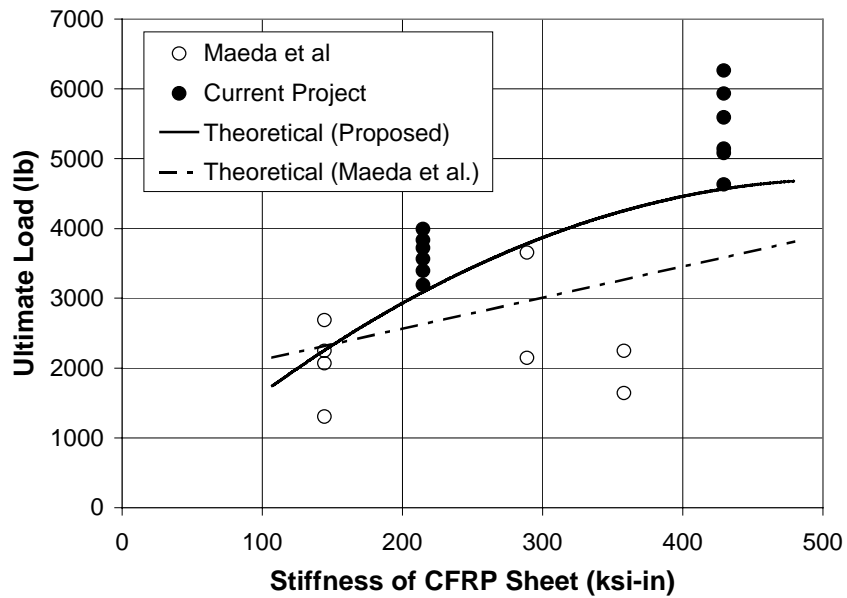
Figure 7: Free-Body Diagram of Sheet with Length dx

To summarize the above discussion, the key equations of the model are shown below. Since only a limited range of stiffnesses has been tested thus far, limits were placed on the equations. These limits can be removed once more testing has been conducted. Using these equations, the ultimate load was plotted versus the stiffness of the sheet (see Figure 8). Also shown on the graph are the experimental values of load versus stiffness. It can be seen that the loads for the current research are higher than the values shown by Maeda et al. (1997). This can be explained by the results of research by Horiguchi and Saeki (1997). They reported that the shear test, which is the test used by Maeda et al. (1997), produces lower ultimate loads than the flexure test.

$$L_e = 3.0 \text{ in} \quad (200 \text{ ksi-in} < n t_f E_f < 450 \text{ ksi-in})$$

$$\tau = [-2.915(n t_f E_f)^2 + 3024(n t_f E_f)] \times 10^{-6} \quad (200 \text{ ksi-in} < n t_f E_f < 450 \text{ ksi-in})$$

$$P_{\max} = \tau \times L_e \times w_f \quad \text{or} \quad f_{fp} = \frac{\tau L_e}{n t_f}$$



Note: 1 lb = 4.45 kN; 1ksi-in = 5.71 GPa-mm

Figure 8: Ultimate Load vs. Stiffness of CFRP Sheet

IMPLICATION ON DESIGN

The significance of the equations is to account for peeling in design. Using the proposed equations, the stress at which peeling would occur can be calculated. This stress would then be used as the ultimate stress in design equations. An example of the calculations is shown below for a single ply of material having a thickness of 0.0065 in (0.165 mm), modulus of elasticity of 33000 ksi (228 GPa), and ultimate tensile strength of 550 ksi (3.79 GPa).

$$L_e = 3.0 \text{ in}$$

$$\tau = -2.915(nt_f E_f)^2 + 3024(nt_f E_f)$$

$$\tau = -2.915(1 \times 0.0065 \text{ in} \times 33000 \text{ ksi})^2 + 3024(1 \times 0.0065 \text{ in} \times 33000 \text{ ksi}) = 0.5145 \text{ ksi}$$

$$f_{fp} = \frac{\tau L_e}{nt_f}$$

$$f_{fp} = \frac{0.5145 \text{ ksi} \times 3.0 \text{ in}}{1 \times 0.0065 \text{ in}} = \underline{\underline{237 \text{ ksi}}}$$

It should be noted that due to recent findings, it is understood that this value of peeling stress is dependent on the surface preparation of the concrete (Miller, 1999). More research is needed to address the influence of the surface preparation.

CONCLUSIONS

The bond between CFRP sheets and concrete is a important issue when using CFRP to repair concrete structures. A summary of an experimental project that addressed the bond along with the following conclusions were presented.

- The bonded length did not have any affect on the ultimate load of the sheet due to the existence of an effective bond length.
- The concrete strength did not affect the ultimate load because the failure occurred in the concrete-adhesive interface.
- Increased FRP stiffness did increase the bond strength, but not proportional to the number of plies.

A model was developed from the experimental results. This model was used to predict the stress at which peeling occurred. This stress can be used in design as the ultimate stress. Limitations were placed on the model due to the range of stiffnesses that were tested. After more research has been conducted, the limitations can be removed from the equations.

ACKNOWLEDGEMENTS

The authors would like to acknowledge NSF for the funding of this project under grant CMS 9796269 and Master Builders Technologies for supplying material.

REFERENCES

Brosens, Kris and Van Gemert, Dionys, (1997). "Anchoring Stresses between Concrete and Carbon Fibre Reinforced Laminates," *Proceedings of the Third International Symposium on Non-Metallic (FRP) Reinforcement for Concrete Structures, Vol 1*, Japan Concrete Institute, Japan, pp. 271-278.

Horiguchi, Takashi and Saeki, Noboru, (1997). "Effect of Test Methods and Quality of Concrete on Bond Strength of CFRP Sheet," *Proceedings of the Third International Symposium on Non-Metallic (FRP) Reinforcement for Concrete Structures, Vol 1*, Japan Concrete Institute, Japan, pp. 265-270.

Maeda, Toshiya; Asano, Yasuyuki; Sato, Yasuhiko; Ueda, Tamon; and Kakuta, Yoshio, (1997). "A Study on Bond Mechanism of Carbon Fiber Sheet," *Proceedings of the Third International Symposium on Non-Metallic (FRP) Reinforcement for Concrete Structures, Vol 1*, Japan Concrete Institute, Japan, pp. 279-286.

Miller, Brian, (1999). "Bond Between Carbon Fiber Reinforced Polymer Sheets and Concrete," MSc Thesis, Department of Civil Engineering, The University of Missouri-Rolla, Rolla, MO, pp. 138.

Nanni, Antonio, (1997). "Carbon FRP Strengthening: New Technology Becomes Mainstream," *Concrete International: Design and Construction, Vol. 19, No. 6*, pp. 19-23.